Journal of Interdisciplinary Mathematics
ISSN: 0972-0502 (Print), ISSN: 2169-012X (Online)
Vol. 28 (2025), No. 1, pp. 183–193
DOI : 10.47974/JIM-1848

Gas sensor for NH_3 and NO_2 gases : Analyzing optical dielectric constants in real and imaginary domains

Abeer S. Alfayhan *
Nahida B. Hasan †
Department of Physics
College of Science
University of Babylon
Babylon 51002
Iraq

Abstract

In this work, thin-film sample preparation was performed using the pulse laser deposition method used pressure around 5 tons of CZTS to make pellets. We prepared the films using a neodymium-YAG laser with an energy of 700 mJ. We created the plasma plume by using a number of pulses (200, 250, 300, 350, and 400) at a rate of 6 Hz. calculated the optical constants, including the refractive index, extinction coefficient, and dielectric constant, for the prepared films. The extinction coefficient and refractive index both go up. The behavior of (εr) is similar to that of the refractive index (n) because (k2) is less than (n2), but (εi) is mostly affected by the value of the extinction coefficient (k). At operational temperatures (250 oC), the films were tested as gas sensors against NH3 and NO2 gases. Additionally, the sensitivity of films to these gases decreases with increasing temperatures. The fluctuation in the operating temperature of the films has significantly reduced the sensor's sensitivity, causing this alteration. At its operational temperature, the gas sensor displayed a gradual increase in response time but a steady decrease in recovery time.

Subject Classification (2020): *34A25.*

Keywords: *Extinction coefficient, Refractive index, Real and imaginary parts, CZTS, Operation temperature, Sensitivity, Recovery, Response, Gas sensor.*

* *ORCID-ID:* 0009-0009-5555-5090
† *ORCID-ID:* 0009-0001-8904-7029

* *E-mail:* abeer_msc@yahoo.com (Corresponding Author)
† *E-mail:* Sci.nahidabukheet@uobabylon.edu.iq

1. Introduction

Many industries require gas sensors for worker and environmental safety. Monitoring for human and environmental harm requires the monitoring of ammonia (NH3) and nitrogen dioxide (NO2). Infectious air pollution kills 3.8 million people annually. Pollution causes 20% of heart disease and stroke deaths [1]. ZTS is quaternary Cu2ZnSnS4. Kieserite-type thin-film solar cells may replace CdTe and CIGS. CZTS compound traits.Due to its direct bandgap of 1.0-1.5 eV, CZTS absorbs many solar wavelengths. CZTS may be an efficient solar absorber because of this. Copper, zinc, tin, and sulfur abound in CZTS [2]. This outperforms rare-element materials in sustainability and cost. Its high absorption coefficient makes CZTS efficient at light absorption. Solar cells benefit from low light reflection. This compound has garnered attention for optoelectronics, solar cells, and gas sensing. CZTS may make a good NH3 and NO3 gas sensor. To detect gas, the p-type semiconductor CZTS absorbs gases and changes electricity flow [3]. CZTS gas sensors recognize NH3 with high sensitivity and selectivity. Transport, industry, and agriculture emit NH3, a major pollutant. At room temperature, CZTS gas sensors detect low NH3 concentrations. In NO3 gas detection, CZTS-based sensors look promising. NO3 matters [4, 13-17].

1. Experiments

Pulsed laser deposition produces nanoscale Cu2ZnSnS4 films. Films were applied to glass substrates by 200, 250, 300, 350, and 400 pulse Nd-YAG lasers at 700 mJ, 6 Hz, 1064nm wavelength, and 10-5 mbar pressure. Flood the container with alcohol after washing the glass slides with 99.9% pure laboratory ethanol. Ultrasonic ate the container for 15 minutes to remove oil impurities. Use a soft cloth or special cleaning paper to prepare the container. Use film after cleaning. We used a UV-Visible Spectrophotometer 2700 to measure CZTS films' real and imaginary transmittance spectra and optical dielectric constants. Interdigitated electrodes. Gas sensors measure thin film resistivity changes from NH3 and NO2 exposure. A k-type thermocouple (XB 9208B) measures temperature. Farell E350 power supplies bias voltage. 8845A/8846A The Fluke Digital Multimeter measures resistance. We tested CZTS thin films on glass substrates for gas operating temperature sensitivity using active voice.

2. Results and Discussion: Optical Properties

1. *Extinction Coefficient*

As it passes through the medium, electromagnetic wave interactions and exponential decay determine the extinction coefficient. Figures (1a) and (1b) display the extinction coefficient, photon energy, and pulse number of CZTS films. The extinction coefficient increases with copper zinc tin sulfide (CZTS) laser pulses for several reasons: Changing the surface: Laser pulses melt, ablate, or oxidize CZTS materials. Modifying surface morphology can cause electronic structure defects, increasing light scattering and absorption. Absorption and scattering increase the extinction coefficient. Powerful laser pulses can alter CZTS's crystalline lattice. Grain growth, phase transitions, and defects are structural changes. The extinction coefficient increases with refractive index and absorption fluctuations.

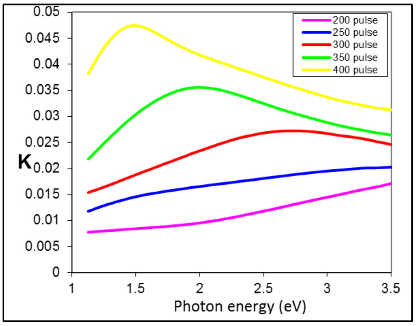

Figure 1a

Extinction coefficient as a function of photon energy(ev) for CZTS films.

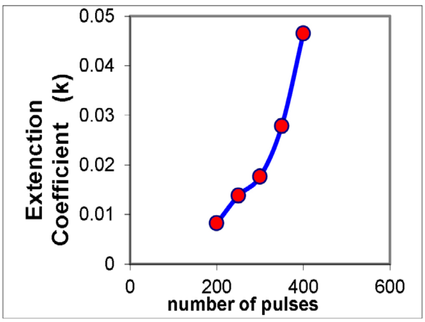

Figure 1b

The extinction coefficient with number of pulses for CZTS films

2. *Refractive Index.*

Figures (2a) and (2b) show CZTS film refractive index versus photon energy (ev) at different laser pulses. The figure shows that laser pulses increase the refractive index (n). Increased laser pulses for CZTS (Copper Zinc Tin Sulfide) cause laser-induced crystallization and a higher index of refraction [5]. Laser pulses generate high-intensity localized heat in CZTS. CZTS melts and cools quickly due to this intense heat. CZTS material forms crystalline structures during cooling, increasing its index of refraction. Crystalline CZTS have a higher density than amorphous or non-crystalline ones, increasing the index of refraction. The density difference changes light propagation speed, increasing the index of refraction. Thus, more laser pulses form more crystalline structures in CZTS, raising its index of refraction.

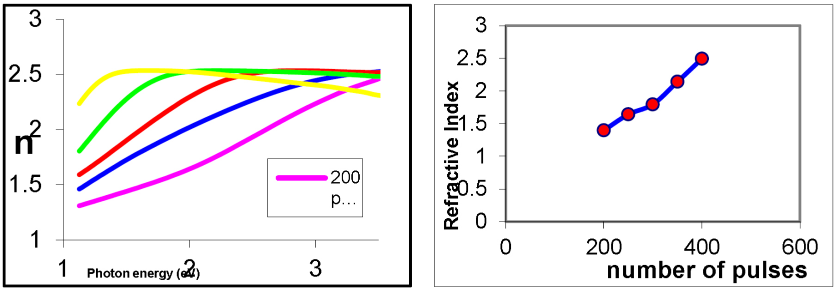

Figure 2

(2a) The variation of the refractive index versus photon energy (ev) for CZTS films, (2b): refractive index with number of pulses for CZTS films.

3. *Real and Imaginary Parts of Optical Dielectric Constant*

Figures (3) and (4) show the real (ε′) and imaginary (ε′′) dielectric constants for CZTS films prepared at various laser pulses (200, 250, 300, 350, and 400) at 1064 nm. To measure real (ε′) and imaginary (ε′) dielectric constants in thin films, use relationships (1 and 2). The behavior of (ε′) is similar to the refractive index (n) due to the smaller value of (k2) compared to (n2), while (ε′) relies on the Extinction Coefficient (k) value.

$$N = n - ik \qquad (1)$$

Where:(n) is the real part of the refractive index. One can calculate the extinction coefficient (K) using the equation [6]:

$$k = \alpha\lambda / 4\pi \qquad (2)$$

Where:(λ) is the wavelength of the incident ray.

The material dielectric constant measures electric field energy storage. The dielectric constant's real (ε′) part stores energy through polarization, while the imaginary (ε′) part dissipates energy through conductivity. There are several ways laser pulses increase CZTS compound real and imaginary dielectric constants: Laser pulses excitonize CZTS electrons. Energy level occupancy boosts material polarization response and the real dielectric constant. Carrier generation: laser pulses increase CZTS electron and hole charge carriers through multiphoton absorption, or carrier multiplication. Extra carriers boost conductivity and the imaginary dielectric constant. Nonlinear effects: High-intensity laser pulses can cause the optical Kerr effect and two-photon absorption in CZTS. Nonlinear effects can raise real and imaginary dielectric constants by changing the material's refractive index. The dielectric constant rise is controlled by the laser pulse's strength, length, the properties of the CZTS compound, and how the laser interacts with matter.

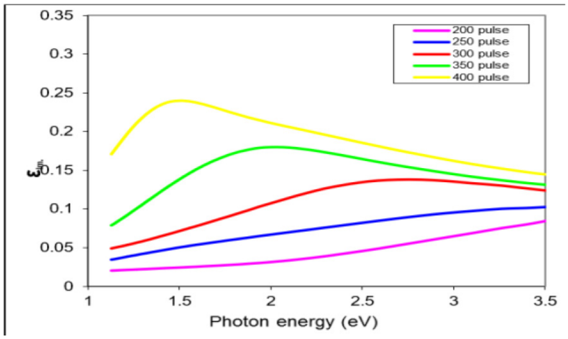

Figure 3

Real dielectric constant as a function of wavelength for CZTS films at different pulses laser (200,250,300,350,400), wavelength (1064) nm.

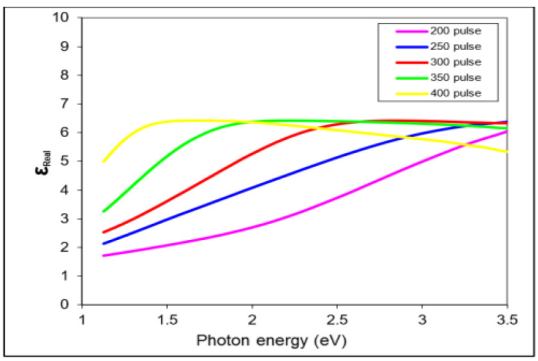

Figure 4

Imaginary dielectric constant as a function of wavelength for CZTS films at different pulses of laser (200, 250, 300, 350, 400), wavelength (1064) nm.

2. Operation Temperature of Sensor

Gas concentration, sensor, and environment determine the best NH3 and NO2 sensor temperature. These gases' sensors' operating temperatures can be calculated using general guidelines. Many 25°C-50°C sensors detect NO2 and NH3. A 25°C experiment can reach 5-10°C. Find the ideal temperature. Oxidizers and oxygen-chemisorbed surfaces indicate gas. Chemically and physically absorb film oxygen. Heating aids in chemisorption. Warmer temperatures activate chemisorption and physisorption. Sensor surface oxygen adsorption rises with temperature [7]. FIGURES 5A-6E show 200-300 °C sensor sensitivity. The NO3-NH3-NH3-mixed ratio and 6-volt electrode bias were used in all sensing tests. Figures 5A-5E show NH3. Temperature reduces sensitivity in all films, but 300-pulse is more sensitive. Diffusion limitations have many causes. By diffusion, sensor surfaces detect gas molecules. Gas molecule diffusion and environmental sensing material equilibrium increase with temperature. Fast diffusion lowers sensor surface gas molecule concentration and sensitivity. The surface area-to-volume ratio decreases with CZTS compound grain size [8]. The lower surface area lets NH3 molecules interact. Fewer adsorption and reaction sites reduce vessel gas sensitivity [9]. Figures 6A-6E show NO2. All films become more temperature-sensitive, but 300-pulse films are more so. Gas NO2 sensitizes metal oxide films to 300 pulses. Metal oxide surfaces oxidize NO2 with CZTS. Smaller CZTS grains increase surface-to-volume ratios and NO2 gas sensitivity. More-surfaced vases are NO2-sensitive. Surface area increases NO2 sensitivity by increasing gas adsorption and reaction sites. [10].

Environmental gases activate gas sensors. The sensor's time to reach a certain percentage of its final output signal, or gas concentration, from baseline to a specified level is usually measured. Gas sensors return to baseline after exposure. Sensor stability and sensitivity recover after gas

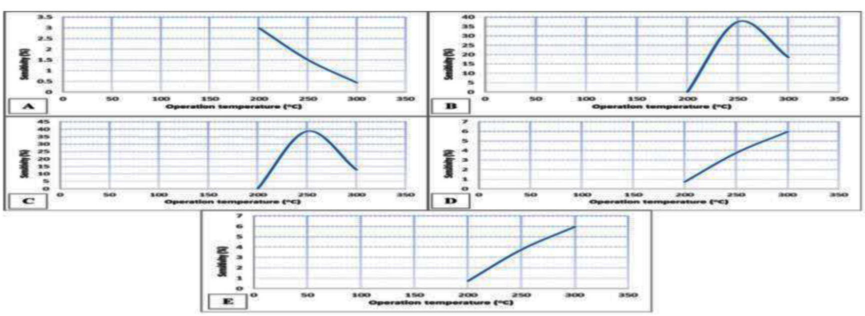

Figure 5

CZTS thin film sensitivity variation with operating temperature, laser pulses (NH3: air), and bias voltage of 6V on glass substrate.

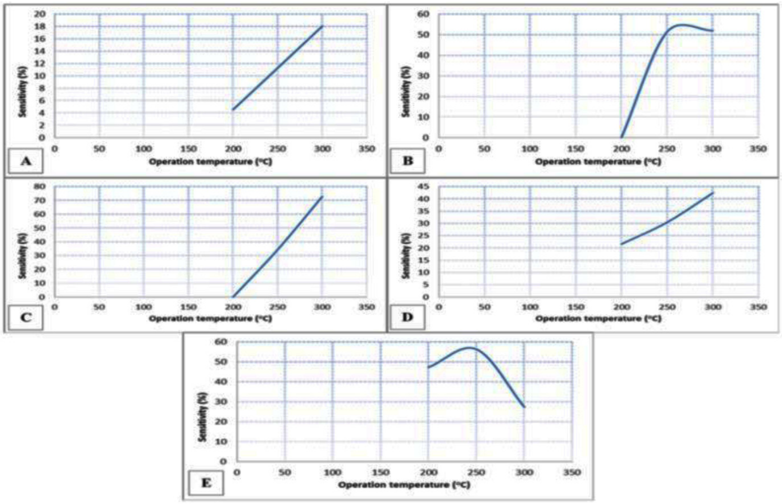

Figure 6

CZTS thin film sensitivity variation with operating temperature, laser pulses (NO2: air), and bias voltage of 6V on glass substrate.Response Time and Recovery Time.

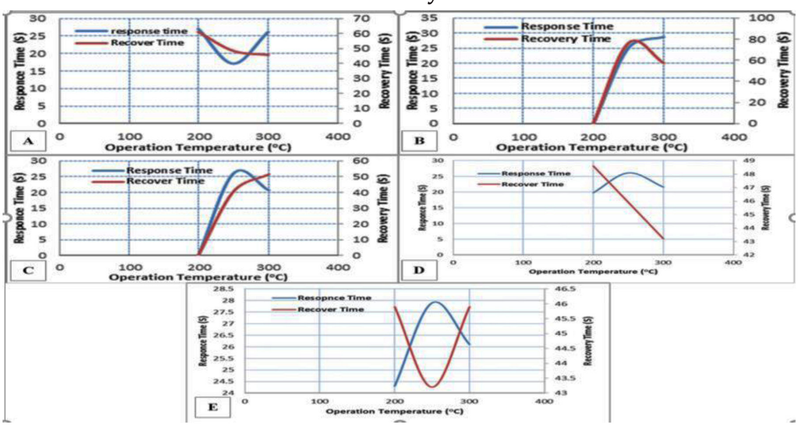

Figure 7

Shows the CZTS thin film response and recovery times for NH3 gas with temperature (oC).

detection. Sensor response and recovery times determine gas concentration detection speed and accuracy. Better sensors recover faster [11]. 6V bias voltage, NH3 gas, and CZTS thin film reactions and recovery times are shown in Figures 7A-7E. Increased Vol.% increases reaction time and decreases recovery time at 200-300 oC (Table 1). Work at low temperatures slowed recovery. Lower temperatures attract O2 species. O- and O- are volatiler than diesel. Figures (8A-8E) show NO2 reaction and recovery times. The CZTS compound-based NO2-gas sensor may recover quickly if its return time is shorter than its response time. Several NO2 measurements help. CZTS compounds remove NO2 or regenerate this sensor's sensing layer [12].

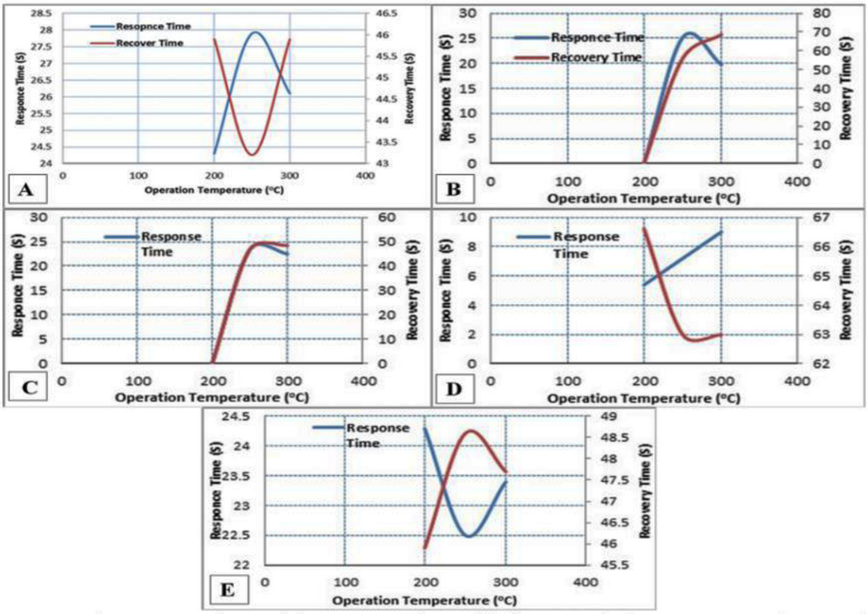

Figure 8

The response time and the recovery time with the Temp.(oC) temperature of CZTS thin films for NO2 gas.

Sample	Response Tim(s) at (200-250-300) °C with NH_3gas	Recovery Time (s) at (200-250-300) °C with NH_3gas	Response Tim(s) at (200-250-300) °C With NO_2gas	Recovery Time (s) at (200-250-300) °C With NO_2gas
	27	61.2	5.4	90 66.6
$CZTS_{200pules}$	17.1	48.6	21.6	49.5
	26.1	45.9	27.9	42.3
	0	0	5.4	66.6
$CZTS_{250pules}$	25.2	76.5	21.6	49.5
	28.8	57.6	27.9	42.3
	0	0	0	0
$CZTS_{300pules}$	26.1	40.5	23.4	46.8
	20.7	51.3	22.5	48.6
	19.8	48.6	5.4	66.6
$CZTS_{350pules}$	26.1	45.9	7.2	63
	21.6	43.2	9	63
	24.3	45.9	24.3	45.9
$CZTS_{400pules}$	27.9	43.2	22.5	48.6
	26.1	45.9	23.4	47.7

Conclusion

Dielectric optical The real and imaginary constants of all pulsed laser deposition films increase with laser pulses. Gases NO2 and NH3 are tested at 200-300 °C. We study sample sensitivity, response time, recovery time, and selectivity. The CZTS thin films produced were strong sensor candidates. Films tested NH3 and NO2 sensors. Temperature decreases film gas sensitivity. Film temperature fluctuations have reduced sensor sensitivity. At operational temperature, gas sensor reaction time increased gradually, but recovery time decreased.

References

[1] G. Abdi, L. Alluhaibi, E. Kowalewska, T. Mazur, K. Mech, A. Podborska, and K. Szaciłowski, "Reservoir computing and photoelectrochemical sensors: A marriage of convenience," *Coordination Chemistry Reviews,* vol. 487, p. 215155, Jul. (2023). [Online]. Available: https://doi.org/10.1016/j.ccr.2023.215155.

[2] S. M. Kadham, "Acute interstitial pneumonia image enhancement using fuzzy partial transforms," *Applied Geomatics,* vol. 16, no. 1, pp. 35–39 (May 2023), doi: https://doi.org/10.1007/s12518-023-00509-8.

[3] A. Sharmin, M. S. Bashar, M. Sultana, and S. M. Al Mamun, "Sputtered single-phase kesterite Cu2ZnSnS4 (CZTS) thin film for photovoltaic applications: Post annealing parameter optimization and property analysis," *AIP Advances,* vol. 10, no. 1 (2020).

[4] N. M. Shinde, P. R. Deshmukh, S. V. Patil, and C. D. Lokhande, "Development of polyaniline/Cu2ZnSnS4 (CZTS) thin film based heterostructure as room temperature LPG sensor," *Sensors and Actuators A: Physical,* vol. 193, pp. 79-86 (2013).

[5] V. Korede, N. Nagalingam, F. M. Penha, N. van der Linden, J. T. Padding, R. Hartkamp, and H. B. Eral, "A review of laser-induced crystallization from solution," *Crystal Growth Design,* vol. 23, no. 5, pp. 3873-3916 (2023).

[6] G. Burns, Solid State Physics, Sections 18-5 and 18-6 (1985).

[7] R. B. Shinde, N. S. Padalkar, S. V. Sadavar, A. S. Patil, S. B. Kale, V. V. Magdum, and J. L. Gunjakar, "Lattice engineering route for self-assembled nanohybrids of 2D layered double hydroxide with 0D isopolyoxovanadate: Chemiresistive SO2 sensor," Materials Today Chemistry, vol. 24, p. 100801 (2022).

[8] M. A. Mustafa, M. A. M. M. Rahman, S. M. S. Islam, S. M. A. R. Iqbal, and A. M. A. S. Hossain, "A novel fuzzy M-transform technique for sustainable ground water level prediction," *Appl. Geomatics,* vol. 16, no. 1, pp. 9–15 (Jan. 2023), doi: 10.1007/s12518-022-00486-4.

[9] S. M. Kadham, M. A. Mustafa, N. K. Abbass, and S. Karupusamy, "Comparison between of fuzzy partial H-transform and fuzzy partial Laplace transform in x-ray images processing of acute interstitial pneumonia," *International Journal of System Assurance Engineering and Management*, Vol 2023, pp 1-9 (2023), doi: https://doi.org/10.1007/s13198-023-02001-3.

[10] P. Wang, T. Wang, F. Li, D. Li, Y. Yang, H. Yu, and X. Dong, "Enhanced sensing response of the first polyoxometalate electron acceptor modified MoS2 for NO2 gas detection at room temperature," *Sensors and Actuators B: Chemical,* vol. 382, p. 133495 (2023).

[11] Y. Wang, X. Fu, T. Wang, F. Li, D. Li, Y. Yang, and X. Dong, "Polyoxometalate electron acceptor incorporated improved properties of Cu2ZnSnS4-based room temperature NO2 gas sensor," *Sensors and Actuators B: Chemical,* vol. 348, p. 130683 (2021).

[12] Y. Wang, T. Wang, H. Shao, F. Li, D. Li, Y. Yang, and X. Dong, "First one-dimensional Cu2ZnSnS4-based gas sensor and enhanced performance at room temperature by polyoxometalate electron acceptor," *Sensors and Actuators B: Chemical*, vol. 380, p. 133405 (2023).

[13] S. Shafiee Alamoti, M. Alaeiyan, and A. R. Gilani, "Studying thermodynamic properties of linear acenes molecules (C4n+2H2n+4) using hyper-Zagreb index," *J. Discrete Math. Sci. Cryptography*, vol. 22, no. 7, pp. 1261-1268 (2019). [Online]. Available: https://doi.org/10.1080/09720529.2019.1694258.

[14] A.M. Darweesh, R.H. Hasan, and S.M. Kadham, "Results of Fourth-Order Differential Superordination and Subordination for Univalent Functions Defined by Integral Operator," *Mathematical Modelling and Engineering Problems*, vol. 11, no. 2, pp. 385–392 (Feb. 2024), doi: https://doi.org/10.18280/mmep.110210.

[15] S. Hussain, F. Afzal, D. Afzal, M. Cancan, S. Ediz, and M. R. Farahani, "Analyzing the boron triangular nanotube through topological indices via M-polynomial," *J. Discrete Math. Sci. Cryptography,* vol. 24, no. 2, pp. 415-426 (2021). [Online]. Available: https://doi.org/10.1080/09720529.2021.1882158.

[16] W. Gao and M. R. Farahani, "The hyper-Zagreb index for an infinite family of nanostar dendrimer," *J. Discrete Math. Sci. Cryptography,* vol. 20, no. 2, pp. 515-523 (2017). [Online]. Available: https://doi.org/10.1080/09720529.2016.1220088.

[17] W. Gao, L. Shi, and M. R. Farahani, "Szeged related indices of TUAC6[p, q]," *J. Discrete Math. Sci. Cryptography,* vol. 20, no. 2, pp. 553-563 (2017). [Online]. Available: https://doi.org/10.1080/09720529.2016.1228312.

Received June, 2024